ARTICLE   OPEN

Check for updates

Valproic acid stimulates myogenesis in pluripotent stem cell-derived mesodermal progenitors in a NOTCH-dependent manner

Natacha Breuls[1,7], Nefele Giarratana[1,2,7], Laura Yedigaryan [1], Gabriel Miró Garrido[1], Paolo Carai[3], Stephane Heymans[3], Adrian Ranga[4], Christophe Deroose[5] and Maurilio Sampaolesi [1,6 ✉]

Muscular dystrophies are debilitating neuromuscular disorders for which no cure exists. As this disorder affects both cardiac and skeletal muscle, patients would benefit from a cellular therapy that can simultaneously regenerate both tissues. The current protocol to derive bipotent mesodermal progenitors which can differentiate into cardiac and skeletal muscle relies on the spontaneous formation of embryoid bodies, thereby hampering further clinical translation. Additionally, as skeletal muscle is the largest organ in the human body, a high myogenic potential is necessary for successful regeneration. Here, we have optimized a protocol to generate chemically defined human induced pluripotent stem cell-derived mesodermal progenitors (cdMiPs). We demonstrate that these cells contribute to myotube formation and differentiate into cardiomyocytes, both in vitro and in vivo. Furthermore, the addition of valproic acid, a clinically approved small molecule, increases the potential of the cdMiPs to contribute to myotube formation that can be prevented by NOTCH signaling inhibitors. Moreover, valproic acid pre-treated cdMiPs injected in dystrophic muscles increase physical strength and ameliorate the functional performances of transplanted mice. Taken together, these results constitute a novel approach to generate mesodermal progenitors with enhanced myogenic potential using clinically approved reagents.

INTRODUCTION

Muscular dystrophies (MDs) are a debilitating group of muscle disorders for which no cure exists. Patients not only suffer from progressive deterioration of the skeletal muscles, leading to a decreased walking ability, but also develop severe cardiomyopathy later on [1]. Therefore, these patients would benefit from a cellular therapy capable of targeting both striated muscle types. Induced pluripotent stem cells (iPSCs) have a high proliferative capacity and can differentiate towards all three embryonic lineages. These characteristics make iPSCs an attractive cell type for regenerative medicine. Furthermore, through differentiation towards mesoderm, bipotent stem cells can be generated. Recently, a first protocol was developed to generate human iPSC-derived mesodermal progenitors (MiPs) by means of embryoid body (EB) formation and subsequent sorting for CD44, CD140A, and CD140B [2, 3]. The obtained MiPs had the in vitro and in vivo ability to differentiate towards both the cardiac and skeletal muscle lineages. Nevertheless, improvements are needed for further translation. Firstly, the use of EBs is very laborious and

heterogeneous, making it necessary to perform subsequent sorting, thus limiting their translatability. Furthermore, MiPs derived from fibroblasts had a much lower myogenic potential than those derived from myogenic progenitors such as mesoangioblasts (MABs) [3]. As fibroblasts are easier to obtain and thus a more attractive source to generate iPSCs, strategies need to be developed to overcome this difference.

The NOTCH signaling pathway is a highly conserved communication system known to be important for myogenesis during embryonic development and postnatal regeneration [4]. Furthermore, stimulation of Delta-like 1 (DLL1)/NOTCH1 has shown to stimulate the regenerative capacity of MABs [5]. In previous studies, the NOTCH1 pathway could be activated through the addition of valproic acid (VPA) [6, 7]. VPA is a small molecule known for its function as a histone deacetylase inhibitor (HDACi). Interestingly, VPA has shown to stimulate myogenesis by both myogenic progenitors and iPSCs [8, 9].

In this study, we aimed to derive human MiPs through a fully chemically defined monolayer approach, thereby enhancing their

[1]Laboratory of Translational Cardiomyology, Department of Development and Regeneration, Stem Cell Research Institute, KU Leuven, 3000 Leuven, Belgium. [2]Stem Cell Laboratory, Department of Pathophysiology and Transplantation, Università degli Studi di Milano, Milano, Fondazione IRCCS Ca' Granda Ospedale Maggiore Policlinico, Centro Dino Ferrari, via F. Sforza 35, 20122 Milano, Italy. [3]CARIM School for Cardiovascular Diseases, Department of Cardiology, Maastricht University, 6229 ER Maastricht, the Netherlands; Department of Cardiovascular Sciences, KU Leuven, 3000 Leuven, Belgium. [4]Laboratory of Bioengineering and Morphogenesis, Biomechanics Section, Department of Mechanical Engineering, KU Leuven, Leuven, Belgium. [5]Department of Nuclear Medicine, University Hospital KU Leuven, Leuven, Belgium. [6]Human Anatomy Unit, Department of Public Health, Experimental and Forensic Medicine, University of Pavia, 27100 Pavia, Italy. ✉email: maurilio.sampaolesi@kuleuven.be
Edited by I. Amelio

clinical translatability. Furthermore, we asked whether the NOTCH signaling pathway can be used to stimulate the myogenic potential of these newly developed chemically defined MiPs (cdMiPs). Thus, we provided evidence that VPA stimulated NOTCH1 in cdMiPs and lead to an increased myogenic potential in a translatable manner.

MATERIALS AND METHODS
Cell culture and differentiation
iPSCs and cdMiPs. Episomal human iPSCs (ThermoFisher Scientific; Pailsey, UK) and sendai-virus iPSCs were cultured on matrigel-coated plates (GeltrexTM LDEV-Free, ThermoFisher Scientific) in Essential 8™ medium (ThermoFisher Scientific) and maintained under normoxic conditions in a humidified incubator. Differentiation towards cdMiPs was based on the first four days of a myogenic differentiation protocol, previously described by Shelton et al. [10]. Briefly, one hour prior to differentiation, iPSCs were incubated with RevitaCell™ Supplement (100X, ThermoFisher Scientific). Afterwards, PSCs were seeded single-cell on Corning® Matrigel® Matrix-coated plates (VWR, Leuven, Belgium) at a density of 50,000 cells/cm². The following day, differentiation was induced by Essential 6TM Medium (ThermoFisher Scientific) supplemented with CHIR99021 (8 µM, Axon Medchem, Groningen, Nederland) for two days. Afterwards, cells were cultured in Essential 6TM medium for another two days. Small molecules such as VPA (1 mM, Sigma, Saint-Louis, MO, USA) or DAPT (20 µM, Tocris, Bristol, UK) were added from day 2–4. Prior to in vivo injections, cells were exposed to 20% FBS for the last 24 h of differentiation.

Co-culture with C2C12 myoblasts and rat cardiomyocytes. C2C12 myoblasts (Sigma) were maintained under hypoxic conditions in a humidified incubator on collagen-coated plates (Sigma). C2C12 growth medium consisted of Dulbecco modified Eagle's minimal essential medium (DMEM, 1X, 4.5 g/L D-glucose, L-glutamine) supplemented with 10% FBS, 1% penicillin–streptomycin (pen–strep) and 1% sodium pyruvate, all from ThermoFisher Scientific [11]. Co-culture with cdMiPs was performed in a 5:1 ratio (cdMiPs:C2C12) on collagen-coated plates (Sigma). The next day, differentiation was induced through culture in DMEM (1X, 4.5 g/L D-glucose, L-glutamine) with 2% horse serum (HS) and 1% pen–strep for five days.

Neonatal rat cardiomyocytes were harvested from new-born rat pups within 24 h after birth (P179/2013). The minced hearts were digested in ADS buffer (tissue culture water supplemented with 0.0085% NaCl, 0.0005% KCl, 0.00015% monohydrated NaH₂PO₄, 0.00125% monohydrated MgSO₄, 0.00125% glucose, and 0.00595% HEPES) supplemented with 0.4% collagenase II and 0.6% pancreatin (all from Sigma). Herein, the hearts were incubated three times for 20 min in a 37 °C-warmed water bath, with continuous shaking. Afterwards, the rat cardiomyocytes were purified using a Percoll gradient (0.458 g/ml to 0.720 g/ml; GE Healthcare, Chicago, USA). Co-cultures with cdMiPs were performed in a 10:1 ratio (cdMiPs: cardiomyocytes) in high-glucose DMEM supplemented with 18% medium 199, 5% HS, 5% FBS, 1% pen–strep, and 1% L-glutamine (all from ThermoFisher Scientific) on gelatin-coated plates (Bio-connect, Huissen, Nederland).

Differentiation towards mesodermal lineages. For both smooth muscle [12] and osteogenic [13] differentiation, 30,000 cells/cm² were seeded single-cell on collagen-coated plates. To induce smooth muscle differentiation, cells were put in DMEM (1X, 4.5 g/L D-glucose) supplemented with 1% pen–step, 1% L-Glutamine, 1% sodium pyruvate, 2% HS (all from ThermoFisher Scientific), and transforming growth factor beta 1 (TGFβ1) (50 ng/ml; Peprotech, New Jersey, USA). For osteogenic differentiation, cells were exposed to αMEM supplemented with 10% FBS, 1% L-Glutamine, 1% pen–strep (all from ThermoFisher Scientific), 50 µM Ascorbic-2-phosphate, 10 mM β-glycerolphosphate, and 10 mM dexamethasone (all from Sigma). Full myogenic differentiation of the cdMiPs was performed according to the protocol published by Shelton et al. [10].

Generation and validation reporter line
The plasmid contained a puromycin resistance cassette (puro), enhanced GFP (eGFP), firefly luciferase (Fluc), and the human sodium iodide symporter (hNIS). Expression was driven by the cytomegaloviral (MLV) early enhancer element together with the chicken beta-actin promoter (CAGGS-promoter). The plasmid was integrated via ZFNs downstream of

exon 1 of the PPP1R12C gene on chromosome 19. Here, iPSCs were resuspended in nucleofection solution 2 (Amaxa; Lonza) with 10 µg of donor plasmid and 3 µg of ZFN messenger RNA per 2×10^6 cells. Integration was performed through electroporation (Program F16, Amaxa). After a week of puro selection, individual clones were expanded.

To check for reporter gene incorporation, genomic DNA was extracted using the PureLink™ Genomic DNA Mini Kit (Thermo Fisher), following the manufacturer's protocol. A PCR was performed to check for the 3′ junction (TTCACTGCATTCTAGTTGTGG and AAGGCAGCCTGGTAGACA) and 5′ Random integration (GTACTTTGGGGTTGTCCAG and TTGTAAAACGACGGCC AG). For Southern Blot analysis, 5 µg of genomic DNA was digested with NcoI (New England Biolabs, Massachusetts, US) and loaded onto a 0.7% agarose gel. Fragments were transferred to a nylon membrane (Zeta-Probe; Biorad) that was ultraviolet-crosslinked, and a pre-hybridization was performed. The probe targeting the homology arm was labeled using the Ladderman Labelling kit (TaKaRa, Shiga, Japan) by PCR using the donor vector. Hybridization of the membrane with the probe was performed using the ExpressHyb™ Hybridization solution (TaKaRa).

In vitro tracer uptake experiment
iPSCs were plated on a 24-well plate under normal growth conditions. Cells were rinsed and incubated for one hour with 250 µl of $^{99m}TcO_4^-$ (0.74 MBq/ml in DMEM; ThermoFisher Scientific). A blocking experiment was performed with the addition of NaClO₄ (0.74 MBq/ml $^{99m}TcO_4^-$ in 10 µM NaCl₄ + DMEM). Afterwards, cells were washed thrice with ice-cold phosphate-buffered saline (PBS; ThermoFisher Scientific), thereby collecting the supernatants. Next, cells were lysed using Reagent A100 lysis buffer and Reagent B Stabilising Buffer (ChemoMetec A/S, Allerød, Denmark) and collected separately from the supernatant. Radioactivity of both the supernatant and the cells was measured by the 2480 Wizard2 Automatic Gamma Counter (PerkinElmer, Waltham, MA, USA). Uptake values were adjusted for tracer decay and corrected for cell amount.

In vitro bioluminescent imaging
iPSCs were exposed to 0.3 mg/l D-luciferin (Promega, Benelux, Leiden, The Nederlands). Images were obtained immediately after D-luciferin application with the IVIS® Spectrum (Caliper Life Science, Hopkington, MA, USA). Photon flux (p/s) was measured and images were further analyzed with Living Image version 4.2 (Caliper Life Science).

Integration doxycycline-inducible DLL1
A doxycycline (dox)-inducible *DLL1* was integrated by means of RMCE. The master cell line (H9) used for RMCE was generated previously using ZFN-mediated integration of a flippase (FLP) recombinase target-flanked donor cassette into the AAVS1 locus [14]. RMCE was performed by nucleofection of the master cell line with a donor vector and the FLPe-expressing vector. Nucleofection was done on 3×10^6 cells obtained after accutase treatment using the hESC Nucleofector Solution Kit 2 (Amaxa) and program F16 using an Amaxa nucleoporator. Donor plasmids were generated through Gibson assembly (NEB) of PCR-amplified open reading frames of the desired genes. Plasmids were then evaluated by digestion and Sanger sequencing. Overexpression of DLL1 was achieved by the addition of 2 µg/ml dox.

Gene expression analysis
Total RNA was extracted using the PureLink™ RNA Mini Kit (Invitrogen) according to the manufacturer's protocol. Afterwards, the RNA was treated with the DNA-free™ Kit (Invitrogen) and 500 ng of RNA was reverse transcribed into cDNA with the Superscript® III Reverse Transcriptase First-Strand Synthesis SuperMix (Invitrogen). Quantitative real-time PCR (qPCR) was performed with the Platinum™ SYBR™ Green qPCR SuperMix-UDG (Invitrogen). The qPCR cycle was performed for 2 min at 95 °C, 40 cycles of 15 s at 95 °C, and 45 s at 60 °C. All primers are listed in Table S1. The obtained Ct values of the tested genes were normalized to the geometric mean of the Ct values of housekeeping genes *RLP13A*, *GAPDH*, and *ACTB*.

Immunostaining
Cells were fixed with 4% paraformaldehyde (Sigma) for 15 min at room temperature. Afterwards, cells were permeabilized with 0.02% Triton (Triton X-100; Sigma) in 1% bovine serum albumin (BSA; Sigma) in PBS (Thermo Fisher Scientific) for 30 min, followed by a 60-min blocking with donkey serum (1:10 diluted in 1% BSA; VWR, Pennsylvania, USA). Incubation with the primary antibody was performed overnight at 4 °C. The following day, cells

were incubated for 1 h with AlexaFluor®-conjugated donkey secondary antibodies (1:500, Thermo Fisher Scientific) and finally counterstained with Hoechst 33342 (20 µm, Thermo Fisher Scientific). Primary antibodies used were: goat anti-OCT4 (1:200; ab27985; Abcam, Cambridge, UK), rabbit anti-NANOG (1:200; ab80892; Abcam), mouse anti-TRA1–60 (1:50; sc-21705; Santa Cruz, Dallas, USA), mouse anti-MyHC (1:20, Hybridoma Bank), rabbit anti-LAMIN A/C (1:300, ab108595, Abcam), rabbit anti-cardiac MyHC antibody (1:100, ab50967, Abcam), rabbit anti-LAMININ (1:300, L9393, Sigma), and mouse anti-sarcomeric alpha-actinin (SMA; 1:100, ab9465, Abcam). Staining with anti-Actin, α-Smooth Muscle - Cy3™ antibody (1:200, C6198, Sigma) was performed for 2 h at room temperature. The presence of calcium deposition after osteogenic differentiation was visualized by incubating the cells with alizarin red S (40 mM, A5533, Sigma, pH4.2) for 10 min. Pictures were taken with an Eclipse Ti microscope (Nikon) by means of Image-Pro Plus 6.0 software (Nikon). Image analysis was performed with ImageJ software (NIH).

Flow cytometry
Cells were diluted to 1×10^6 cells/ml with FACS buffer (2% FBS, 10 mM HEPES, and 10 mM NaN$_3$ at a pH of 7.2, all from ThermoFisher Scientific) and incubated with the primary antibodies for 30 min at 4 °C. The following antibodies were used: CD44-FITC (0.25 µg/10^6 cells, 11-0441-81, Thermo Fisher), CD140a-PE (10 µl/10^6 cells, 558002, BDBioscience, Eysins, Switzerland), and CD140b-APC (5 µl/10^6 cells, A15719, Thermo Fisher). Right before analysis, the cells were stained with SYTOX™ green dead cell stain (1 µl/ ml) to assess viability. UltraComp eBeads™ compensation beads (Thermo Fisher) were used for compensation. The analysis was performed on a BD FACSCanto™ II HTS (BD Biosciences).

Western blot
Cells were lysed using a urea-thiourea buffer (7 M urea, 2 M Thiourea, 4% CHAPS, 0.1% β-mercaptoethanol, and 30 mM Tris HCl pH8.5, all from Sigma) supplemented with cOmplete™ Protease Inhibitor Cocktail (1:100, Thermo Fisher) and phosphostop (1:100, Roche, Basel, Switzerland). Thirty micrograms of protein was dissolved in sample-loading buffer (5% SDS, 0.2% bromophenol blue, 50% glycerol, and 250 mM Tris HCl pH8.5, all from Sigma), loaded onto 10% SDS-polyacrylamide gels and subsequently transferred onto nitrocellulose membranes (Protran, Sigma). Membranes were blocked with tris-buffered saline (TBS) containing 0.05% Tween and 5% skim milk powder (Sigma) and incubated with the primary antibody overnight at 4 °C. The following day, membranes were incubated with the secondary antibody for 1 h at room temperature. All secondary horseradish peroxidase-conjugated antibodies (BioRad) were diluted 1:5000 in TBS-Tween and 2.5% skim milk powder. The polypeptide bands were detected with Gel Doc™ chemiluminescence detection system (BioRad) after incubation with SuperSignal™ West Pico Chemiluminescent substrate (Thermo Scientific, Catalog #34087) or SuperSignal™ West Femto Maximum Sensitivity substrate (Thermo Fisher Scientific, Catalog #34095). Relative densitometry was obtained by normalizing the protein band versus background and a housekeeping protein. The primary antibodies used were rabbit anti-Dll1 (0.5 µg/ml, PA5–42902, Thermo Fisher) and rabbit anti-Cleaved Notch1 (1:500, 4147, Cell Signaling).

In vivo differentiation potential of cdMiPs
Sgcb$^{-/-}$/Rag2γc$^{-/-}$ mice were injected intra-muscularly with either saline or 1.5×10^6 cdMiPs (with or without FBS) in the quadriceps, gastrocnemius, and tibialis anterior. For the cardiac injection, 1.5×10^6 cells were suspended in 30 µl Reduced Growth Factor Basement Membrane Matrix 1:1 diluted in DMEM-F12 and injected in the left ventricle wall. Afterwards, the mice were monitored through bioluminescence imaging (BLI). For in vivo BLI scans, mice were placed in the flow chamber of IVIS® Spectrum. Subsequently, 126 mg/kg of D-luciferin was injected subcutaneously. Next, consecutive frames were acquired until the maximum signal intensity was reached. The grafted muscles were harvested 4 weeks after transplantation, embedded in OCT and snap frozen in liquid nitrogen. Serial transverse 8 µm cryostat sections were obtained from cell-injected muscles using the cryostat (Leica, Wetzlar, Germany).

Functional analyses
We performed three different functional tests on Sgcb$^{-/-}$/Rag2γc$^{-/-}$ dystrophic murine model, as for the previous in vivo experiment. Due to the scarce availability of these mice, after genotyping the 3 different littermates we got 12 double knockout mice ranging between 6 and

9 weeks old from our starting point (day 0). The mice were equally divided for age and sex among three different groups of 4 mice: untreated group (UT) where only saline was injected, cdMiPs-treated group (cdMiPs), and cdMiPs + VPA-treated group (cdMiPs + VPA). Four days before injections, hIPSCs underwent the first 4 days of skeletal muscle differentiation following the same procedure as for the other experiments of the manuscript, forming cdMiPs with and without VPA. 1.5×10^6 cells were resuspended in 120 ul and equally distributed within TA, Q, and GN by intramuscular injection. The day of injection (day 0), all the mice performed our three chosen functional tests as a baseline starting point. Grip strength test, gait analysis, and treadmill exhaustion test were performed in this order, which was always kept along all the timeline of the experiment. Mice were always weighted at the end of the treadmill run. A span of 5 days-time point was set for all the tests and kept for one month.

Treadmill exhaustion test. The test was performed at day 0, 5, 10, 15, 20, 25, and 30 after the beginning of the experiment (day 0). The electric shock frequency and intensity were pulses of 200 msec/pulse of electric current with 2 pulse/sec repetition rate (3 Hz) and intensity (1.22 mA), as indicated by Giarratana et al. [12]. The mice were introduced to the treadmill belt and an adaptation time of 5 min was given before the recordings (motor speed set to zero, for 5 min). A training time of 2 min at 4 m/min was set. Later on, the motor speed was set to 7 m/min, with a 1 m/min increase and a constant uphill inclination of 20°, until exhaustion and >10 s stop. The mice were weighted right after every run. Speed (m/min), distance (m), and time (min and sec) were registered and used for calculating the work of each run in J. The formula here applied was: Work (J) = body mass (kg) x gravity (9.81 m = s2) x vertical speed (m/s x angle) x time (s).

Grip strength test. Grip strength was assessed using a grip strength meter (GSM) consisting of a flat surface force meter (Columbus Instruments, Columbus, Ohio). For forelimb and all limb strength assessment, the animal was allowed to hold the horizontal mesh with either the fore limb paws, or the all limb pows and then was gently pulled back until its grip was broken. The force transducer retained the peak force reached when the animal's grip was broken and is shown on a digital display. This was repeated five times during each session within a 2-minute time-frame. During this procedure the mice generally resisted by grasping the mesh with either the forelimbs or all four limbs. Five successful fore and all limb strength measurements were recorded over a period of 2 min. The maximum values for each day over a 5-day period were used for subsequent analysis. The grip strength measurements were collected in the morning hours over a 5-day period, and data were normalized to body weight and expressed as N/gr.

Gait analysis. The experiment was conducted with one mouse at a time. Black and blue ink, a walkway with walls to the sides, and a paper sheet for the bottom part of the walkway were used. Firstly, the hind limb paws were submerged in blue ink. The fore limb paws were submerged in black ink. Immediately after, the mouse was released at the walkway's start to perform the test. The mouse was expected to move in a straight line. If the behavior was not as wanted (stopping, turning back) an object was used to slightly push the animal in the correct direction. Once the walk was completed the mouse was returned into its respective cage. The paper sheet was also changed. This procedure was managed in the same way for all the mice. The analysis was done taking into consideration the stride length (distance between the centers of two consecutive limb's footprints of the same limb) and the stride width (distance between the stride length line and the footprint's center of the opposed limb) as parameters. This was measured on both the forelimbs and the hindlimbs. Left limb's values were mainly used unless a proper gait analysis could not be done with left limb's data. In that case, right limb's values were used.

The measurement was conducted with a ruler and a pencil. First, measuring and drawing the stride length line. Then, obtaining the stride width using the stride length line. The stride width line starts at the center of the opposite paw and is perpendicular to the stride length line. This was repeated at least five times for each parameter. Afterwards, an average of the parameters' values was obtained.

Single-cell RNA sequencing
CdMiPs were sorted single-cell by FACS in 96-well plates in RLT buffer. mRNA was isolated using the genome and transcriptome sequencing protocol [14]. Prior to isolation, external RNA controls consortium (ERCC) spike-in RNAs can be added to the RLT buffer. Further processing was done
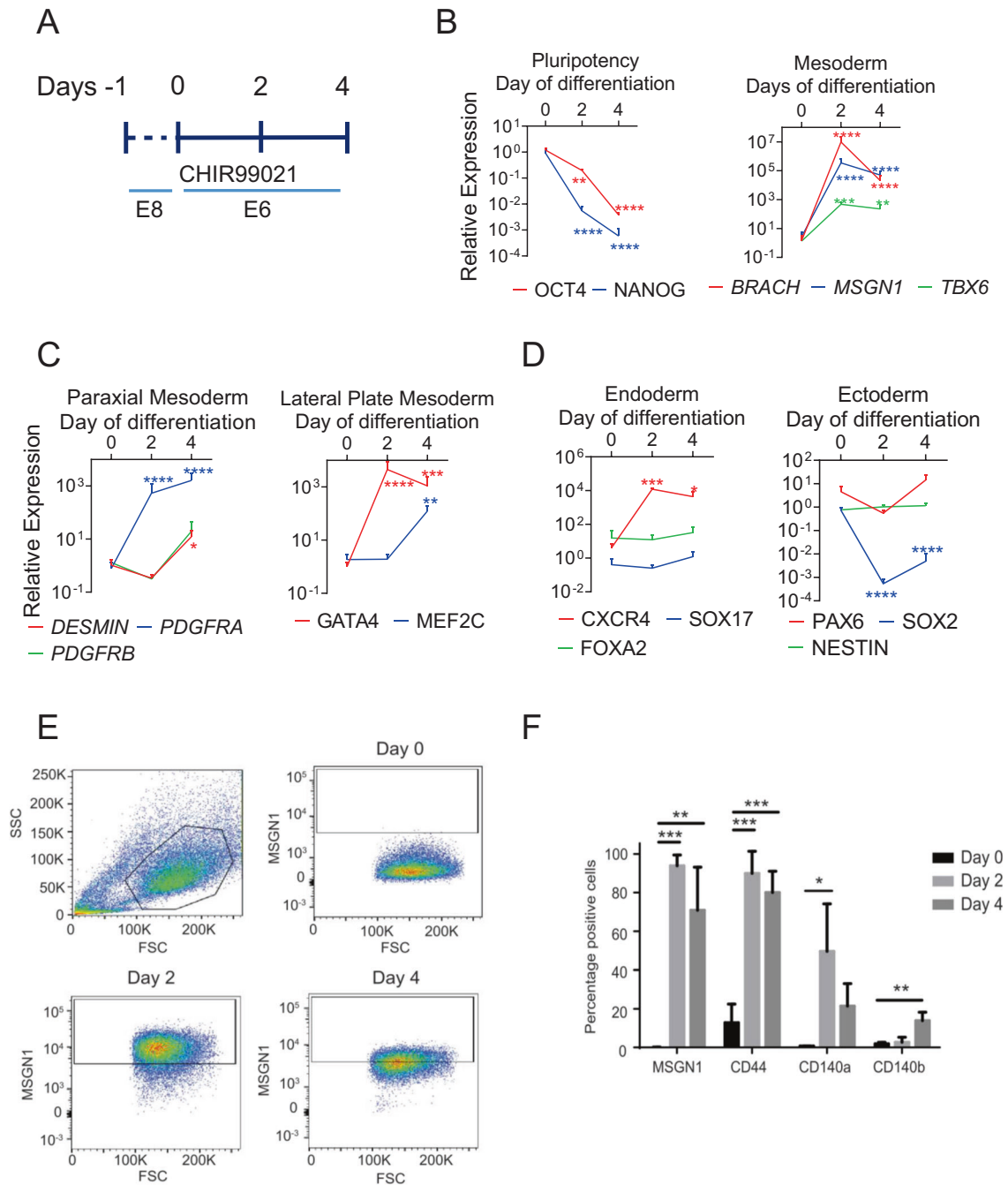
Fig. 1 Mesodermal progenitors can be derived trough a chemically defined monolayer approach. A Schematic overview of the protocol to differentiate induced pluripotent stem cells towards mesodermal progenitors. **B**–**D** Gene expression of markers for pluripotency, early and late mesoderm, ectoderm, and endoderm during mesoderm differentiation. **E** FACS analysis of Mesogenin1 (MSGN1) during differentiation using a MSGN1–2A-Venus reporter line. **F** Percentage of MSGN1, CD44, and CD140A/B positive cells during differentiation, based on FACS analysis. *P < 0.05; **P < 0.01; ***P < 0.001; ****P < 0.0001. $n = 3$–4.

using the Smart-seq2 protocol [15, 16]. Briefly, cells were incubated for 3 min at 72 °C. Afterwards, the RNA was reversely transcribed and amplified via PCR for 25 cycles. Amplification was done with KAPA HIFI Hot Start ReadyMix (KAPA Biosystems, Wilmington, USA) and purified by magnetic beads (CleanNA). Quantity and quality of cDNA were assessed with a Qubit fluorometer (Thermo Scientific) and Agilent 2100 BioAnalyzer, respectively. The libraries were prepared with the Nextera XT library prep and index kit (Illumina). 100 pg of cDNA was tagmented by transposase Tn5 and amplified with dual-index primers (i7 and i5, 14 cycles). In total 279 single-cell libraries were pooled together and sequenced single-end 50 bp on a single lane of a HiSeq4000 (Illumina).

In the Fastq files, tags were trimmed with cutadapt 1.5. The retained tags were aligned to the Ensembl GRC38p7 human reference genome using STAR 2.4.0 [17]. Quality control on aligned and counted reads was done with Scater 1.8.4 [18], cells with less than 150,000 reads; less than 2500 or over 8500 detected genes; less than 6% mitochondrial DNA and less than 10% of spike-in ERCCs were removed. Read normalization was done with Scran 1.8.4. The first ten principal components were used to reduce the dimensionality of the data. Afterwards, t-SNE were computed with a perplexity of 5 in the package Seurat v2.1.0. Clustering was performed with SC3 1.8.0 using $k = 2$–3. Differential expression between clusters was calculated using a likelihood ratio test corrected for multiple testing with a
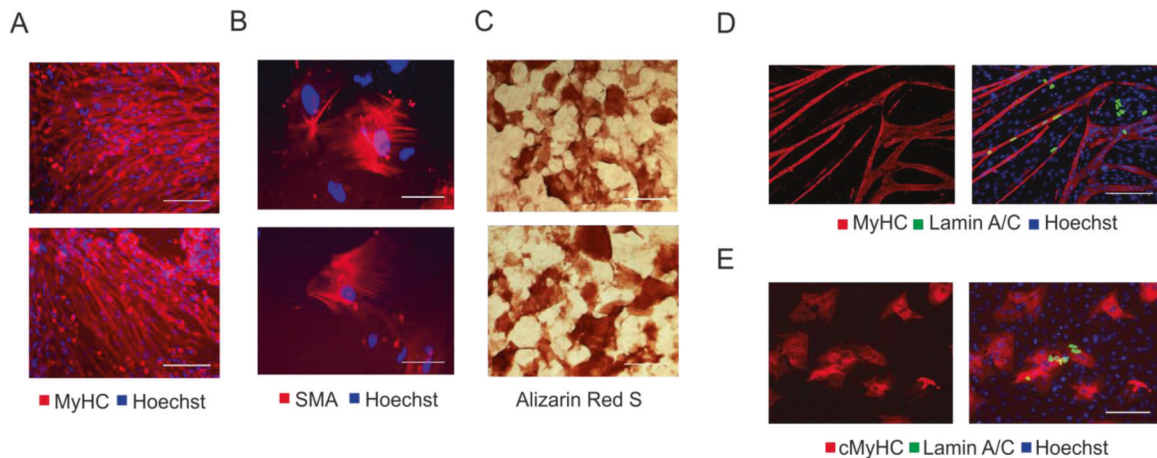
Fig. 2 Mesodermal progenitors have the potential to differentiate towards multiple mesodermal lineages and contribute to in vitro cardiac and skeletal muscle formation. A Immunofluorescence of MyHC (red) after myogenic differentiation. **B** Immunofluorescence after smooth muscle differentiation (SMA). **C** Alizarin red S staining after osteogenic differentiation of the mesodermal progenitors. **D–E** Immunofluorescence analysis of lamin A/C-positive mesodermal progenitors (green) in co-culture with either C2C12 myoblasts **(D)** or rat cardiomyocytes **(E)**. Scale bars: 100 μm.

Benjamini–Hochberg false discovery rate correction with MAST. Marker genes defined as genes with areas under the receiver operating curve (AUROC) > 0.85 and with $P < 0.01$ using SC3 1.8.0 [19]. Data has been deposited in GEO under accession code GSE177048.

Statistical analysis
Statistical analysis and generation of graphs were performed on GraphPad Prism 7.0 (GraphPad Software, San Diego, CA, USA). Two-tailed t test or one-way ANOVA were used to compare interrelated samples, with a Tukey's post-hoc test to correct for multiple comparison. Two-way ANOVA was used for comparing multiple factors. Data is represented as mean ± standard error of the mean (SEM). The number of independent experiments or biological replicates are represented in the figure legends.

RESULTS
Chemically defined mesodermal progenitors have the ability to differentiate into the myogenic and cardiac lineages
In order to obtain cdMiPs, human iPSCs were differentiated for four days following a serum-free monolayer approach (Fig. 1A). During the differentiation, the cells gradually lost pluripotency markers OCT4 and NANOG, while early mesodermal markers such as BRACH, MSGN1, and TBX6 were upregulated after two days of CHIR99021 exposure (Fig. 1B). From day 2 onwards, markers for both paraxial as well as lateral plate mesoderm were upregulated (Fig. 1C). Apart from CXCR4, ecto- and endodermal markers stayed more stable over time (Fig. 1D).

Using a human MSGN1–2A-Venus iPSC line, $93.9 \pm 4.6\%$ of the cells were positive MSGN1$^+$ after two days of differentiation, correlated to a strong mesoderm induction (Fig. 1E) [20]. Furthermore, looking at the markers previously used to isolate MiPs, a higher percentage of CD44, CD140A, and CD140B-positive cells could be observed from day 2 onwards, increased at this stage of differentiation (Fig. 1F).

To confirm the mesodermal nature of our cdMiPs, the cells were differentiated towards skeletal muscle, smooth muscle, and osteogenic lineages. After differentiation, the cdMiPs were positive for myosin heavy chain (MyHC), alpha smooth muscle actin (SMA), and alizarin red S, respectively (Fig. 2A–C). To check whether the cells have the potential to contribute to the myogenic and cardiac lineages, cdMiPs were put in co-culture with either C2C12 myoblasts or rat cardiomyocytes. After subsequent differentiation, the lamin A/C-positive cdMiPs expressed either MyHC ($6.97 \pm 6.19\%$) or cardiac MyHC ($11.72 \pm 14.31\%$) after co-culture with C2C12 myoblasts or rat

cardiomyocytes, respectively (Fig. 2D, E). In general, we were able to produce cdMiPs that have the ability to differentiate into multiple mesodermal lineages.

Mesodermal progenitors show long-term survival and engraftment upon serum exposure
In order to address the in vivo functionality of the cdMiPs, a multifunctional imaging reporter gene construct was integrated via zinc finger nuclease (ZFN)-targeting, downstream of exon 1 of the gene phosphatase 1 regulatory subunit 12 C (PPP1R12C) gene, known as the safe-harbor adeno-associated virus site 1 (AAVS1) locus [21]. The reporter genes were driven by the hybrid CAGGS promoter consisting of an early cytomegalo virus enhancer fused to a chicken beta-actin promoter. The reporter genes used were enhanced green fluorescent protein (eGFP) for immunofluorescence, firefly luciferase (Fluc) for bioluminescence imaging (BLI), and human sodium-iodide symporter (hNIS) for positron emission tomography (PET) (Fig. S1A). Here, the hNIS reporter gene has the benefit of being used already in a clinical setting for tumor detection, and can thus be used in patients for stem cell tracking [22]. A specific integration of the construct into the AAVS1 locus was confirmed via a junction assay and Southern blot analysis (Fig. S1B and C). After the integration, the cells maintained their expression of pluripotency factors OCT4 and NANOG and showed expression of the hNIS reporter gene, Solute Carrier Family 5 Member 5 (SLC5A5) (Fig. S1D). Functional Fluc was validated via BLI (Fig. S1E) and eGFP could be detected via immunofluorescence (Fig. S1F). Furthermore, the uptake of pertechnetate ($^{99m}TcO_4^-$) confirmed functionality of the hNIS. This uptake was completely abolished upon administration of sodium perchlorate ($NaClO_4$), a specific hNIS blocker, confirming specific uptake through the hNIS (Fig. S1G). Once the reporter construct was integrated, 1.5×10^6 cdMiPs were injected into the hind limbs of beta-sarcoglycan-null (Sgcb$^{-/-}$)/ common gamma knockout (Rag2γc$^{-/-}$) mice. After injection, the BLI signal was lost after two days, indicating a low survival rate (Fig. 3A). In order to prepare the cells better for the in vivo environment, fetal bovine serum (FBS) was added to the cdMiPs from day 3–4 of differentiation. Pre-exposure of the cells to 10% FBS led to a higher signal right after injection compared to the untreated cdMiPs. However, this signal was lost seven days post injection (Fig. 3B). When the concentration of FBS was increased to 20%, the cells showed long-term survivability (Fig. 3C). After an initial drop, the BLI signal could be maintained for up to 28 days post injection (Fig. 3D).
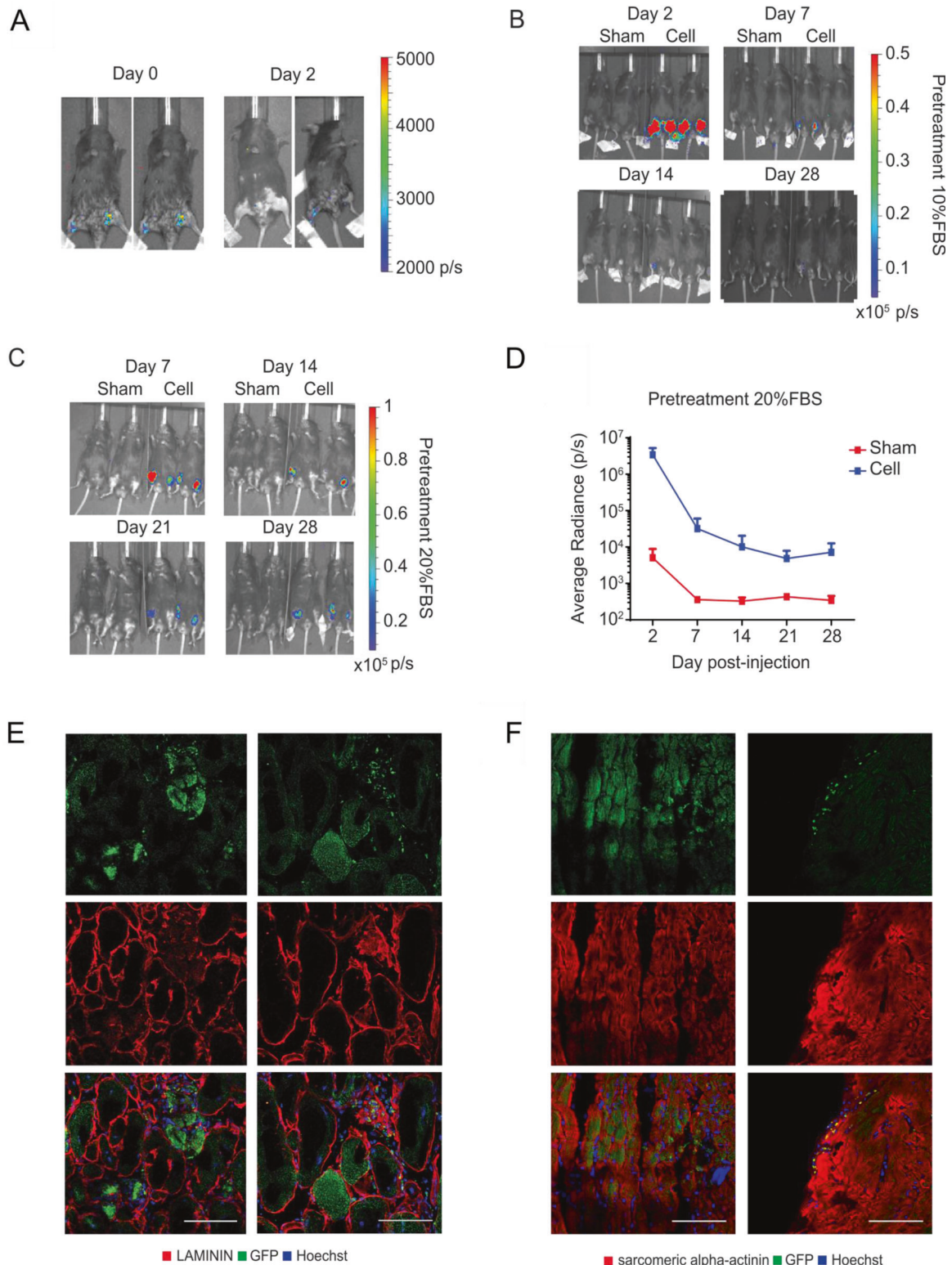
Fig. 3 Serum pre-treatment of mesodermal progenitors leads to long-term survivability and stable engraftment in the skeletal and cardiac muscles. **A** Representative bioluminescent images of beta-sarcoglycan-null ($Sgcb^{-/-}$)/ common gamma knockout ($Rag2\gamma c^{-/-}$) mice injected in both hind limbs with 1.5×10^6 mesodermal progenitors (cdMiPs). **B** Representative bioluminescent images of $Sgcb^{-/-}/Rag2\gamma c^{-/-}$ mice injected with saline (sham) or 1.5×10^6 cdMiPs treated with 10% serum (cell) in the hind limbs. Images were taken 2-, 7-, 14-, and 28-days post injection. **C** Representative bioluminescent images of Sgcb$^{-/-}$/Rag2γc$^{-/-}$ mice injected with saline (sham) or 1.5×10^6 cdMiPs pre-exposed to 20% serum (cell) in the hind limbs. Images were taken 7-, 14-, 21-, and 28-days post injection. **D** Quantification of the BLI signal seen in **C** ($n =$ 3). **E** Immunofluorescent images of the GFP$^+$ cdMiPs present in the skeletal muscle 28 days after injection. **F** Immunofluorescence of the GFP$^+$ cdMiPs present in the heart, 28 days after injection. Scale bars: 100 µm.

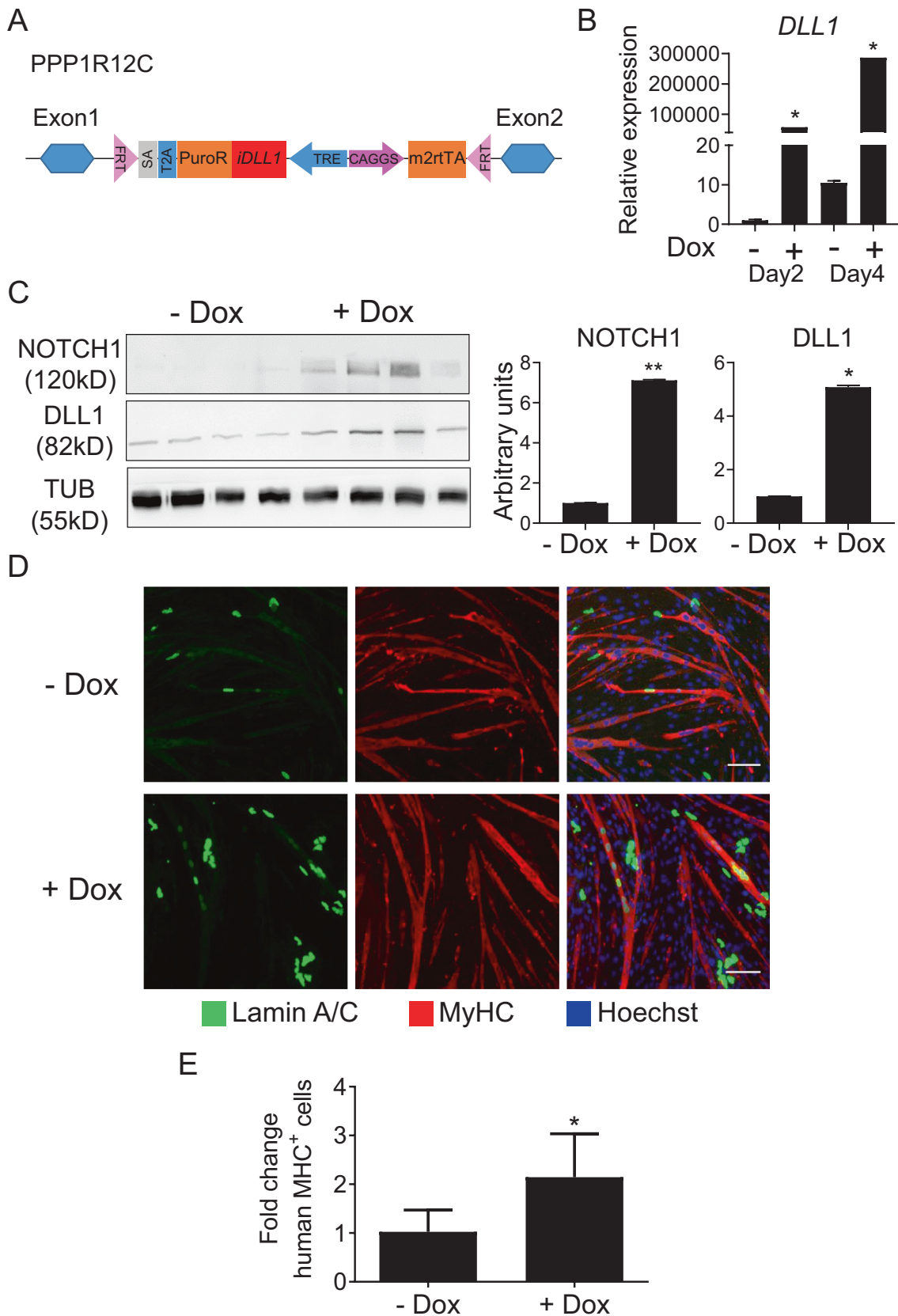**Fig. 4 *DLL1* overexpression improves the myogenic propensity of mesodermal progenitors. A** Schematic overview of the doxycycline (dox)-inducible DLL1 construct flipped into an embryonic stem cell (ESC) master line. **B** Quantitative PCR for *DLL1* after exposure of the generated ESC line to dox for two or four days. **C** Western blot for DLL1 and NOTCH1 after exposure of the generated ESC line to dox for four days. Tubulin (TUB) was used as a housekeeping protein. Quantification graph is on the right. **D** Immunofluorescence analysis of lamin A/C-positive mesodermal progenitors, with or without dox, (green) in co-culture with C2C12 myoblasts (*n* = 3). Scale bars: 100 μm. *P < 0.05.
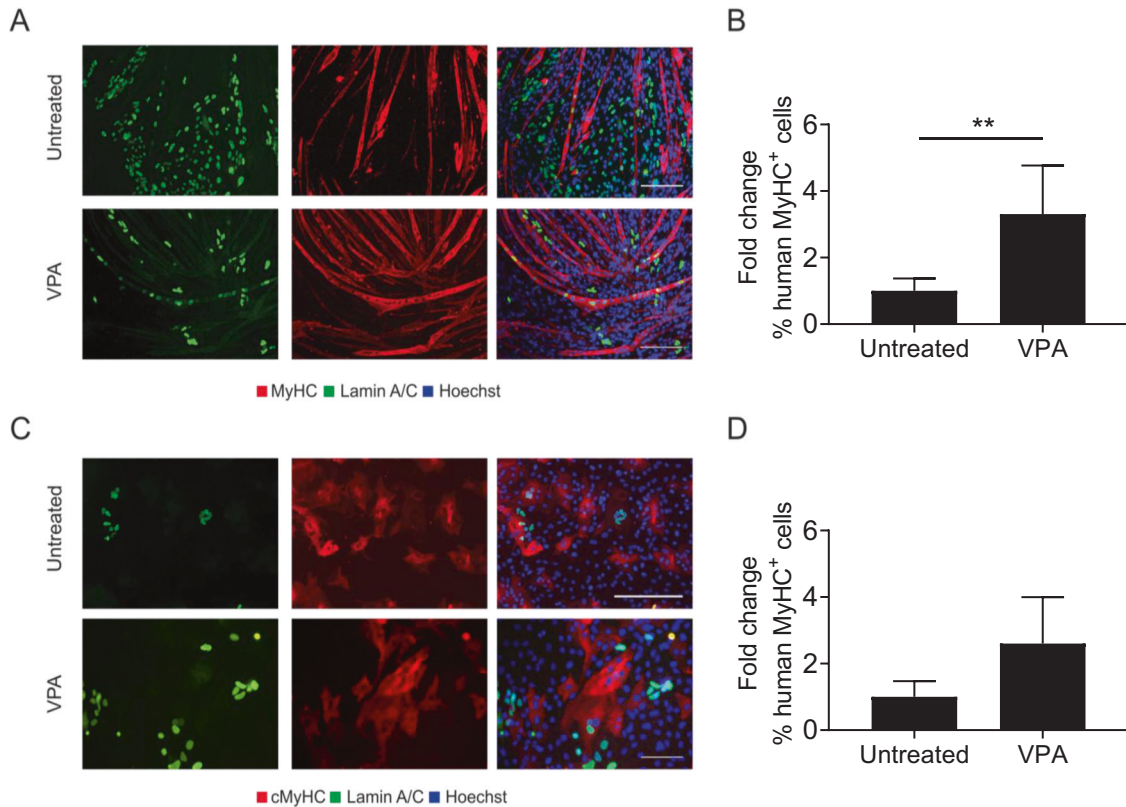
Fig. 5 Valproic acid increases the myogenic potential of mesodermal progenitors while maintaining the cardiogenic potential.
A Immunofluorescence of lamin A/C-positive mesodermal progenitors (green), with or without exposure to valproic acid (VPA) in co-culture with C2C12 myoblasts. **B** Amount of lamin A/C-positive mesodermal progenitors positive for myosin heavy chain (MyHC), compared to the untreated condition ($n = 4$). **C** Immunofluorescence of lamin A/C-positive mesodermal progenitors (green), with or without exposure to VPA, in co-culture with rat cardiomyocytes. **D** Amount of lamin A/C-positive cells positive for cardiac myosin heavy chain (cMyHC), compared to the untreated condition ($n = 3$). Scale bar: 100 μm. ***$P < 0.001$.

Although exposure to serum can introduce heterogeneity in the culture, the addition of 20% FBS did not lead to any changes in the gene expression of key meso-, ecto-, and endodermal markers (Fig. S2). After 28 days, GFP$^+$ cdMiPs could be detected within the muscle fibers of the skeletal muscle. Besides their fusion into existing myofibers, individual GFP$^+$ LAMININ$^+$ cells were detected, indicating differentiation of the cdMiPs into the myogenic lineage (Fig. 3E). To investigate whether the cdMiPs have the ability to engraft in the heart, 1.5×10^6 cdMiPs were injected in the wall of the left ventricle of Sgcb$^{-/-}$/Rag2γc$^{-/-}$ mice. After injection, individual GFP$^+$ sarcomeric alpha-actinin$^+$ cells were detected, indicating differentiation of the cdMiPs towards the cardiac lineage (Fig. 3F). These data reveal that the cdMiPs can engraft in both cardiac and skeletal muscle tissues. However, prior exposure to serum is necessary to guarantee long-term survival upon injection.

NOTCH activation through DLL1 increases the myogenic potential of cdMiPs
Recently, our group identified that induction of the DLL1/ NOTCH1 signaling pathway could enhance the myogenic regenerative capacity of MABs [5, 23]. MABs resemble the generated cdMiPs, as they both can differentiate towards multiple mesodermal lineages and show the expression of CD44, CD140B, and CD140B (Fig. 1). Therefore, we wanted to determine if induction of the NOTCH pathway through DLL1 could improve the myogenic potential of cdMiPs. In order to stimulate the NOTCH signaling pathway, a construct containing a doxycycline (dox)-inducible DLL1 was inserted into a human embryonic stem cell (ESC) master cell line by means of recombinase-mediated cassette exchange

(RMCE) (Fig. 4A) [24]. After integration, a higher amount of DLL1 became apparent after four days of dox treatment and, as a consequence, NOTCH1 was also increased (Fig. 4B, C). Adding dox during the entire mesodermal differentiation led to an increased contribution of these cells to myotubes upon co-culture (Fig. 4D, E). These results suggest that activation of the NOTCH signaling through DLL1 drives cdMiPs towards the myogenic lineage.

Valproic acid relies on the NOTCH signaling pathway to stimulate myogenesis
To use the beneficial effect of NOTCH activation, a small molecule is needed to induce NOTCH signaling in a manner that allows future clinical translation. Previously studies already showed that VPA can stimulate NOTCH1 signaling pathway [6]. Furthermore, VPA has shown to enhance the myogenic capacity of adult stem cells and to induce myogenesis directly in iPSCs [8, 9]. To test its effect on the cdMiPs, 1 mM VPA was added from day 2–4 of differentiation. Afterwards, the cells were put in co-culture with either C2C12 myoblasts or rat cardiomyocytes (Fig. 5). Upon VPA treatment, ~3-fold more lamin A/C-positive nuclei were detected in MyHC$^+$ myotubes, suggesting a beneficial effect of VPA on the myogenic capacity of the cdMiPs (Fig. 5A, B). Additionally, no decrease was detected in the amount of lamin A/C-positive cardiomyocytes after exposure to VPA (Fig. 5C, D). These results suggest that VPA stimulates the myogenic capacity of cdMiPs without interfering with their ability to form cardiomyocytes. In order to investigate whether an initial increase in NOTCH is necessary for the pro-myogenic effect of VPA, γ-secretase inhibitor DAPT was added from day 0–4 of differentiation to inhibit the NOTCH signaling pathway. DAPT prevents cleavage of the NOTCH
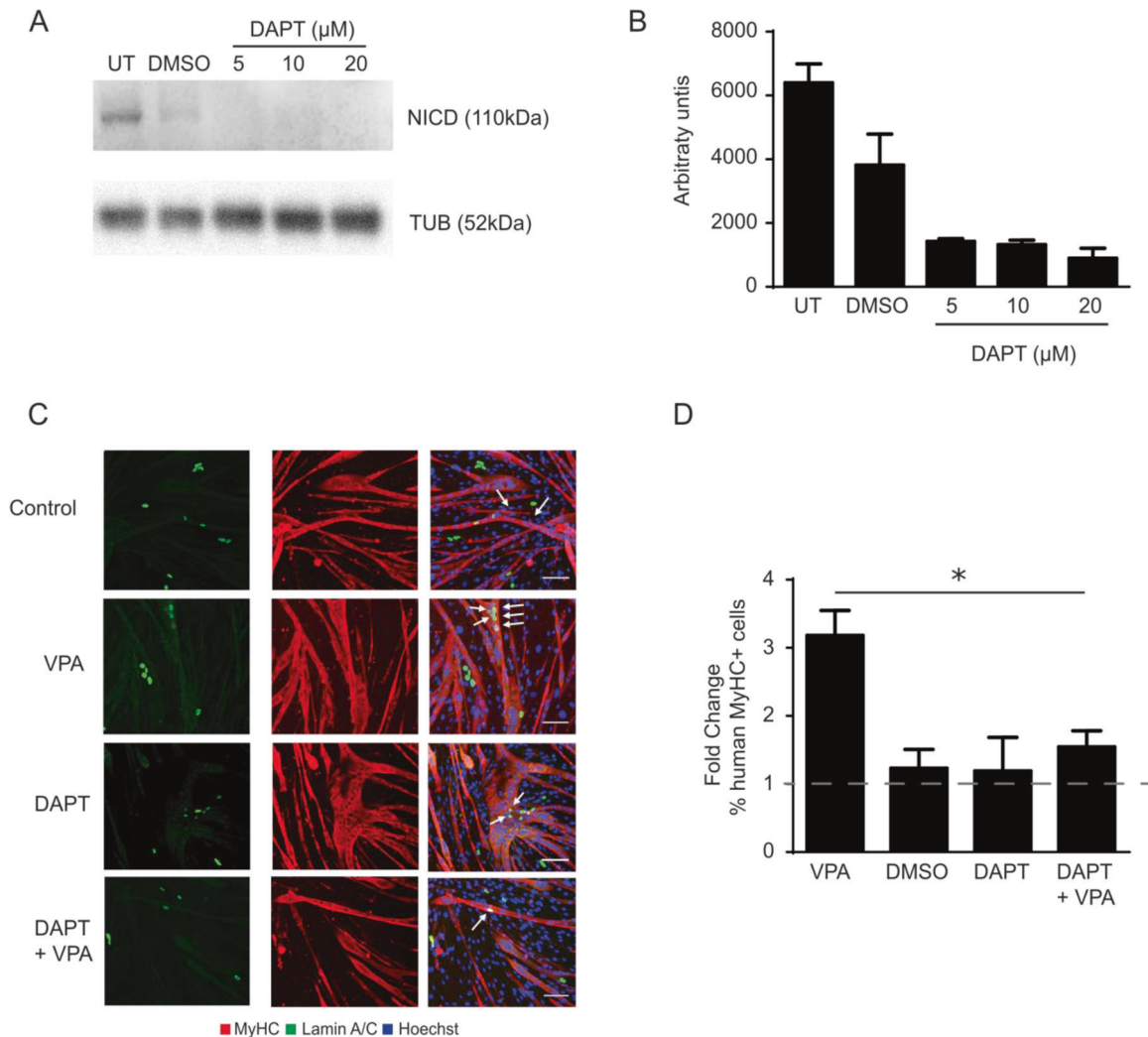
Fig. 6 Activation of the NOTCH signaling is required for valproic acid to stimulate myogenesis. A Representative Western blot for the NICD of mesodermal progenitors exposed to dimethyl sulfoxide (DMSO) or 5, 10, and 20 μM of DAPT from day 0–4 of differentiation. TUB was used for normalization. **B** Quantification of **A**. $n = 2$. **C** Immunofluorescence of lamin A/C-positive mesodermal progenitors (green), untreated or with exposure to VPA, DMSO (control), DAPT or DAPT + VPA, in co-culture with C2C12 myoblasts. **D** Fold change of lamin A/C-positive cells, positive for myosin heavy chain (MyHC) compared to the appropriate control (untreated or DMSO). $n = 3$. Scale bar: 100 μm. *$P < 0.05$.

receptor and thus prevents the release of the NOTCH intracellular domain (NICD). Addition of 5–20 μM DAPT led to a decrease of the NICD (Fig. 6A, B). When DAPT was added during the entire length of the differentiation, no difference could be observed in the amount of lamin A/C$^+$ cells in the MyHC$^+$ myotubes compared to the dimethyl sulfoxide (DMSO)-treated control. However, when DAPT was added together with VPA, the increase normally seen in lamin A/C$^+$ MyHC$^+$ cells, is abolished (Fig. 6C, D). Taken together, it seems that the initial activation of the NOTCH signaling pathway is important for VPA to elicit its pro-myogenic effect.

Valproic acid pre-treated cdMiPs improve functional performances of dystrophic mice

To demonstrate whether VPA treatment has a beneficial effect on muscle strength and performances, we employed three different functional tests (grip strength, gait analysis, and treadmill exhaustion tests) on $Sgcb^{-/-}/Rag2\gamma c^{-/-}$ dystrophic murine model, resembling Limb Girdle muscular dystrophy type 2E. The mice were equally divided for age and sex among three different groups of 4 mice: untreated group (UT), cdMiPs-treated group (cdMiPs), and cdMiPs + VPA-treated group (cdMiPs + VPA). Four

days before injections, hiPSCs underwent the first 4 days of skeletal muscle differentiation and subsequently injected in the respective court. A span of 5 days-time point was set for all the tests and kept for one month (Fig. 7A). The baseline showed at day 0 no differences among all the groups (Fig. 7 A, C, D). The UT mice started to show a functional decline already after 15 days, which affected their muscular strength and activities. The two treated groups improved their performances over time. In particular, the grip strength test showed a significant increase of the normalized force in cdMiPs-treated mice compared to controls that can be even improved by pretreating the cells with VPA (Fig. 7B and Fig. S3A). The stride length of both hind and fore limbs in the gait analysis was higher for cdMiPs and VPA + cdMiPs-treated mice compared to UT, confirming the better performance of VPA-treated mice (Fig. 7C and Fig. S3B). Lastly, treadmill exhaustion test confirmed an amelioration of running performance in cdMiPs and VPA + cdMiPs-treated mice in terms of work, distance, time, and power (Fig. 7D and Fig. S3C). Thus, these results proved a functional amelioration in dystrophic mice transplanted with cdMiPs that can be improved by pretreating progenitors with VPA.
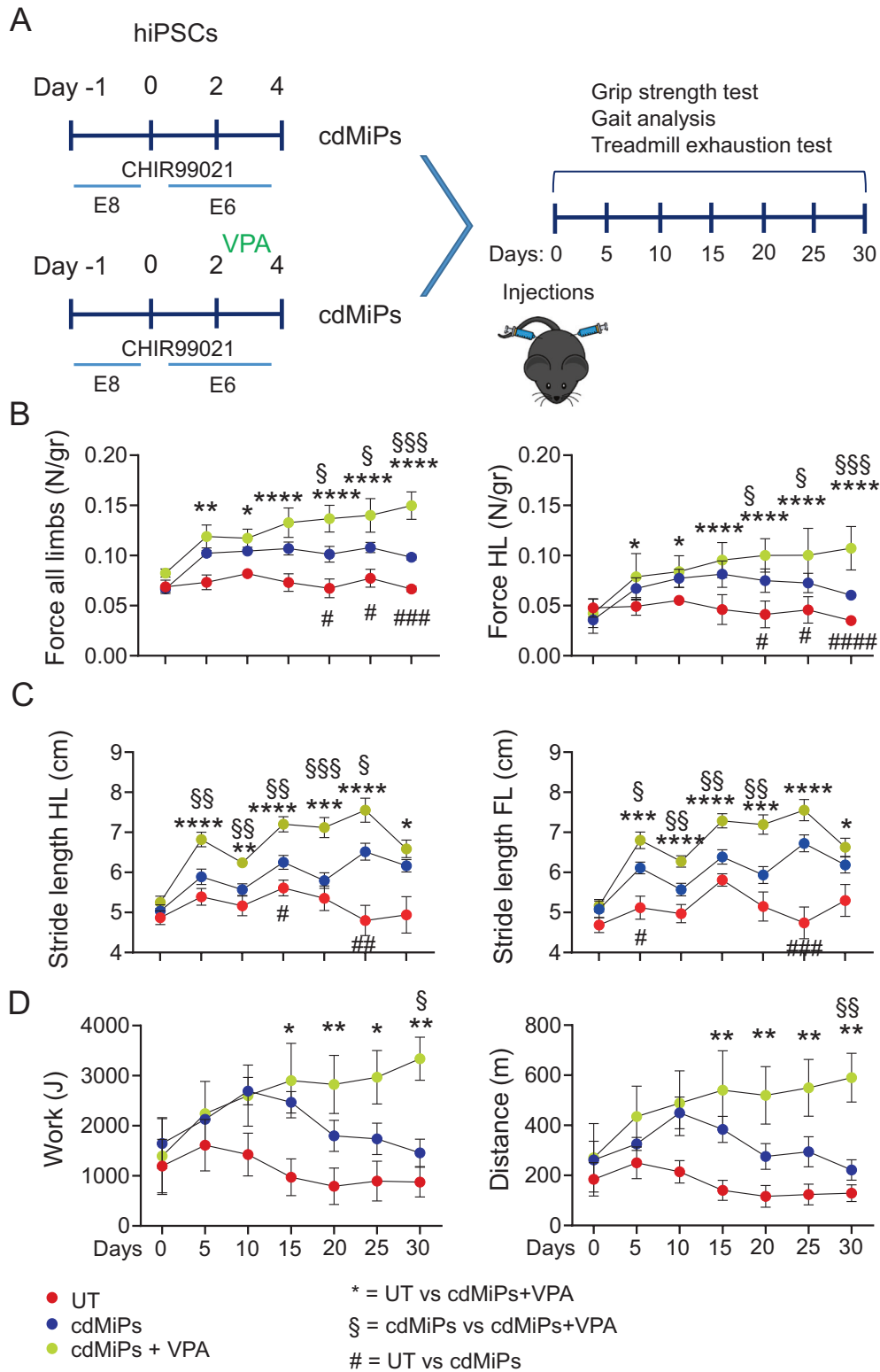
Fig. 7 Valproic acid pre-treated cdMiPs improve functional performances of dystrophic mice. A Timeline illustrating the experiment setup. At day -1, hiPSCs underwent the first 4 days of skeletal muscle differentiation, with and without VPA treatment up to forming cdMiPs. After cell injection, $Sgcb^{-/-}/Rag2\gamma c^{-/-}$ dystrophic mice performed grip strength test, gait analysis, and treadmill exhaustion test at day 0, 5, 10, 15, 20, 25, and 30. **B** Grip strength test for all and hind limbs of UT, cdMiPs, and cdMiPs + VPA-treated mice showed as normalized force calculated as ration between the force (N) and the body weight of each mouse (N/gr). **C** Gait analysis for hind and fore limbs stride length of UT, cdMiPs, and cdMiPs + VPA-treated mice. **D** Treadmill exhaustion test of UT, cdMiPs, and cdMiPs + VPA-treated mice up to one month follow up. From left to right, graphs of Work (J) and Distance (m). All the functional tests were performed at day 0, 5, 10, 15, 20, 25, and 30. $N = 4$. *, § and # $p < 0.05$; **, §§ and ## $p < 0.01$; ***,§§§ and ### $p < 0.001$; ****,§§§§ and #### $p < 0.0001$ by two-way ANOVA. * UT vs cdMiPs + VPA. § cdMiPs vs cdMiPs + VPA. # UT vs cdMiPs.
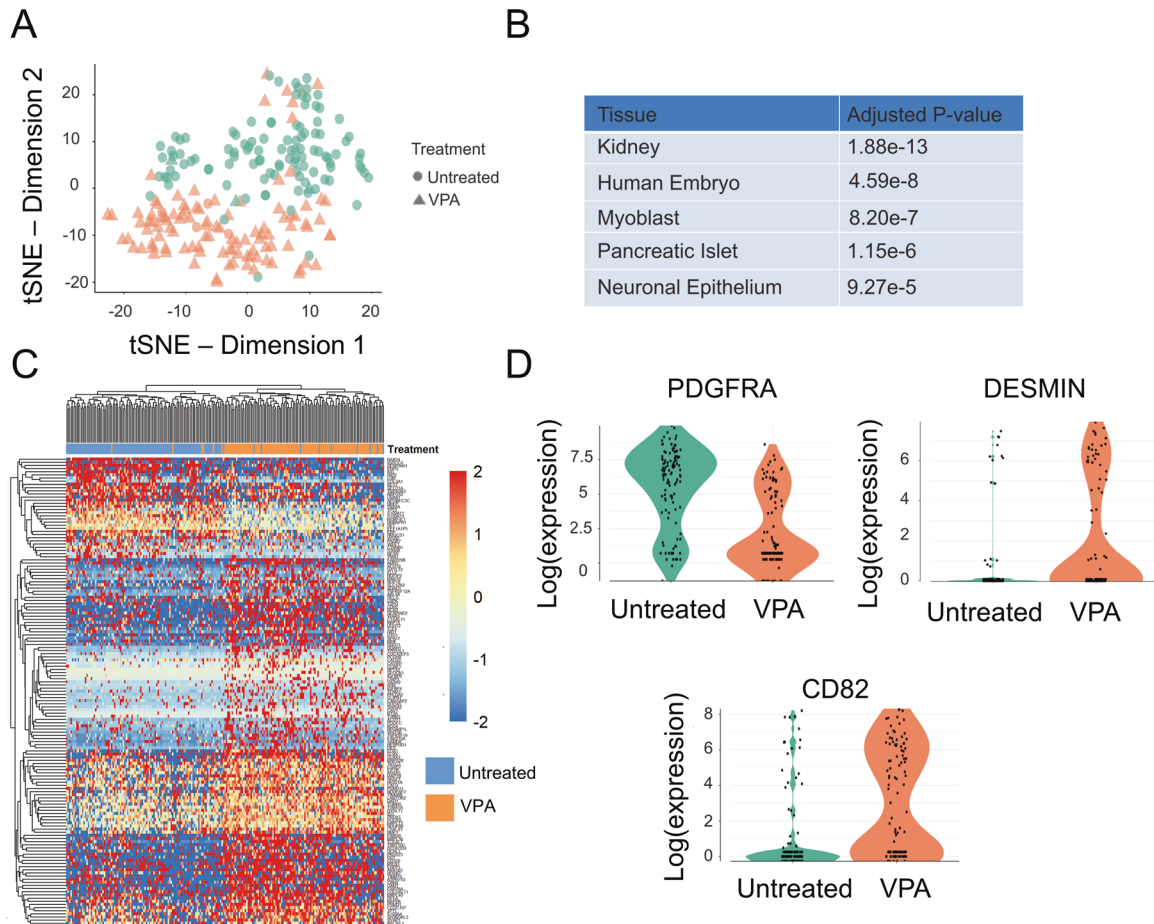
Fig. 8 **Single-cell RNA sequencing reveals an upregulation of myogenic regulators after valproic acid treatment. A** t-SNE plot colored by *k*-means clustering (*k* = 2) of 227 cells either untreated (circles) or treated with valproic acid (VPA, triangles). **B** Top 5 ARCHS4 significantly enriched in the cluster corresponding to the VPA-treated cells. **C** Heatmap of *k*-means clusters with myogenic-related genes differentially expressed between untreated and VPA-treated mesodermal progenitors. **D** Expression of platelet-derived growth factor receptor A (PDGFRA), DESMIN and CD82 in untreated and VPA-treated mesodermal progenitors.

Single-cell RNA sequencing shows that valproic acid pushes cell towards a myogenic state

To unravel the mechanics on how VPA affects the cdMiPs, single-cell RNA sequencing (scRNAseq) was performed of both untreated and VPA-treated cells using SMART-Seq2 (GSE177048) [16]. Afterwards, thorough quality control, we retained 227 high-quality cells (Fig. S4A, B). Upon SC3 clustering, the *t*-distributed stochastic neighborhood embeddings (t-SNE) plot can be divided into three main clusters. The two largest corresponded to the untreated cdMiPs and those exposed to VPA, while the third cluster mainly contained cells in metaphase (Fig. S4C, D). The use of two clusters led to a division that completely depended on the treatment with an even distribution of the cell cycle state, and was used for further analysis (Fig. 8A). We used gene set enrichment analysis to annotate the clusters further with correlations to the ARCHS4 tissues database [25]. Here, we found that the gene expression profile of the VPA-treated group correlated more to myoblasts compared to the untreated group (Fig. 8B, C). Some key myogenic genes found to be differentially expressed were platelet-derived growth factor receptor A (*PDGFRA*), which decreased upon VPA treatment, and *DESMIN* and *CD82*, which were upregulated upon VPA supplementation (Fig. 8D). Since the VPA-mediated myogenic improvement is shown to be NOTCH-dependent, we wondered whether it was due to its transcription modulation. The fact that no relevant NOTCH-related genes and crucial signaling pathways were found in the VPA-treated cells (Fig. S4E, F) excluded this hypothesis. The results of scRNAseq analysis show that VPA treatments increase the number of myogenic progenitors, affecting gene transcription.

DISCUSSION

Dual progenitors targeting both skeletal and cardiac muscles are of great interest to target the most debilitating manifestation of MDs. Recently, our laboratory was the first to develop mesodermal progenitors from iPSCs that could successfully differentiate into skeletal and cardiac lineages both in vitro and in vivo [26]. A recent review provided a blueprint for translational regenerative medicine depicting that successful translation requires manufacturing processes that is reliable and can be scaled while remaining financially viable [27]. In this study, we identified a robust approach to generate mesodermal progenitors. By using chemically defined media and differentiating the cells in a monolayer, we provided a more homogeneous method that can be scaled up more easily.

Despite the fact that the protocol was performed in a serum-free manner, a 24-hour pre-exposure to FBS was needed to guarantee in vivo survival. It has already been shown that serum-deprivation induces apoptosis, suggesting a possible protective effect of serum against cell death [28, 29]. The same was found by Kim et al. who showed a low survivability upon transplantation of myogenic progenitors derived from a serum-free protocol [30]. The addition of serum for 24 h did not lead to any major changes in important lineage markers. However, animal products should

be avoided, as there is a risk of the presence of non-human pathogens that can induce an unwanted immune response and subsequent cell rejection. Human serum has already been used to replace FBS in the field of mesenchymal stem cells [31, 32]. Within the field of MDs, cells were injected into a golden retriever MD model using serum of the recipient dog, leading to significant engraftment [33, 34]. This method could be translated into a human setting, where the patients' own serum can be used to avoid any immune response. The fact that valproic acid pre-treated cdMiPs transplanted in dystrophic mice positively impact muscle strength and functional performances is calling for additional preclinical studies. In this view, some further experiments could be carried out on GRMD dogs [34], the large animal model that better resemble dystrophic signs seen in patients affected by Duchenne muscular dystrophy.

As shown previously for adult stem cells and iPSCs, VPA was able to stimulate the myogenic commitment of our cdMiPs. Indeed, we found that an increase in the induction of the NOTCH signaling pathway is necessary for VPA to exert its effect. Previously, it was reported that VPA could directly stimulate NOTCH1 in carcinoid tumors [6]. On the contrary, our scRNAseq showed no relevant differences in NOTCH-related genes suggesting that although the presence of NOTCH is important for VPA to exert its effect, VPA itself does not directly target the NOTCH genes in cdMiPs. In addition, from our transcriptomic data it is clear that the effect of VPA is not limited to the myogenic lineage, as networks from the embryonic, neuronal, and pancreatic lineages are also upregulated after VPA-treatment. These findings are also confirmed by literature where VPA has been used to stimulate reprogramming and neuronal differentiation [35, 36]. The exact fate that is stimulated thus depends on the environment in which the cells reside. This could pose a problem in vivo where the cells might come in contact with a wide range of signals. VPA is known as a very broad HDACi, leading to this wide variety of effects. Pinpointing the exact mechanism through which VPA exerts its effect on myogenesis, might allow us to find a more specific HDACi with less adverse effects. Here, several other HDACi, including the recently approved Givinostat, have shown to stimulate myogenesis in adult stem cells and thus can be considered within this protocol [37, 38]. Another strategy could be selecting a subpopulation specifically linked to the myogenic lineage. Here, CD82 could be a candidate as it has been identified recently as a novel marker for human satellite cells [15, 39].

Taken together, we have been able to optimize a protocol to generate cdMiPs. Furthermore, we found that VPA improves the myogenic capacity of these cdMiPs. This beneficial effect is mediated through an increase in the induction of the NOTCH signaling pathway. We envision that this novel approach to generate mesodermal progenitors and increase their myogenic potential improves the potential of the cdMiPs to be translated into a form of cell therapy.

REFERENCES

1. Birnkrant DJ, Bushby K, Bann CM, Apkon SD, Blackwell A, Colvin MK, et al. Diagnosis and management of Duchenne muscular dystrophy, part 3: primary care, emergency management, psychosocial care, and transitions of care across the lifespan. Lancet Neurol. 2018;17:445–55. [Research Support, U.S. Gov't, P.H.S. Review]

2. Giacomazzi G, Holvoet B, Trenson S, Caluwe E, Kravic B, Grosemans H. et al. MicroRNAs promote skeletal muscle differentiation of mesodermal iPSC-derived progenitors.Nat Commun. 2017;8:1249 [Research Support, Non-U.S. Gov't]1.

3. Quattrocelli M, Swinnen M, Giacomazzi G, Camps J, Barthélemy I, Ceccarelli G, et al. Mesodermal iPSC-derived progenitor cells functionally regenerate cardiac and skeletal muscle. J Clin Invest. 2015;125:4463–82.

4. Mayeuf-Louchart A, Lagha M, Danckaert A, Rocancourt D, Relaix F, Vincent SD. et al. Notch regulation of myogenic versus endothelial fates of cells that migrate from the somite to the limb. Proc Natl Acad Sci USA. 2014;111:8844–9. [Research Support, Non-U.S. Gov't]17.

5. Quattrocelli M, Costamagna D, Giacomazzi G, Camps J, Sampaolesi M. Notch signaling regulates myogenic regenerative capacity of murine and human mesoangioblasts. Cell Death Dis. 2014;5:e1448 [Research Support, Non-U.S. Gov't] 9.

6. Greenblatt DY, Vaccaro AM, Jaskula-Sztul R, Ning L, Haymart M, Kunnimalaiyaan M. et al. Valproic acid activates notch-1 signaling and regulates the neuroendocrine phenotype in carcinoid cancer cells. Oncologist. 2007;12:942–51. [Research Support, N.I.H., Extramural Research Support, Non-U.S. Gov't].

7. Sahakyan V, Pozzo E, Duelen R, Deprest J, Sampaolesi M. Methotrexate and valproic acid affect early neurogenesis of human amniotic fluid stem cells from myelomeningocele. Stem Cells Int. 2017;2017:6101609.

8. Iezzi S, Di Padova M, Serra C, Caretti G, Simone C, Maklan E, et al. Deacetylase inhibitors increase muscle cell size by promoting myoblast recruitment and fusion through induction of follistatin. Dev Cell. 2004;6:673–84.

9. Li Q, Foote M, Chen J. Effects of histone deacetylase inhibitor valproic acid on skeletal myocyte development. Sci Rep. 2014;4:7207.

10. Shelton M, Kocharyan A, Liu J, Skerjanc IS, Stanford WL. Robust generation and expansion of skeletal muscle progenitors and myocytes from human pluripotent stem cells. Methods. 2016;101:73–84. [Research Support, Non-U.S. Gov't]15.

11. Ronzoni FL, Giarratana N, Crippa S, Quattrocelli M, Cassano M, Ceccarelli G, et al. Guide cells support muscle regeneration and affect neuro-muscular junction organization. Int J Mol Sci. 2021;22:1939.

12. Giarratana N, Conti F, La Rovere R, Gijsbers R, Carai P, Duelen R, et al. MICAL2 is essential for myogenic lineage commitment. Cell Death Dis. 2020;11:654. 2020/ 08/18

13. Ceccarelli G, Presta R, Lupi SM, Giarratana N, Bloise N, Benedetti L, et al. Evaluation of poly(lactic-co-glycolic) acid alone or in combination with hydroxyapatite on human-periosteal cells bone differentiation and in sinus lift treatment. Molecules. 2017;22:2109.

14. Macaulay IC, Teng MJ, Haerty W, Kumar P, Ponting CP, Voet T. Separation and parallel sequencing of the genomes and transcriptomes of single cells using G&T-seq. Nat Protoc. 2016;11:2081–103. [Research Support, Non-U.S. Gov't].

15. Camps J, Breuls N, Sifrim A, Giarratana N, Corvelyn M, Danti L. et al. Interstitial cell remodeling promotes aberrant adipogenesis in dystrophic muscles. Cell Rep. 2020;31:107597–5.

16. Picelli S, Faridani OR, Bjorklund AK, Winberg G, Sagasser S, Sandberg R. Full-length RNA-seq from single cells using Smart-seq2. Nat Protoc. 2014;9:171–81. [Research Support, Non-U.S. Gov't].

17. Dobin A, Davis CA, Schlesinger F, Drenkow J, Zaleski C, Jha S, et al. STAR: ultrafast universal RNA-seq aligner. Bioinformatics. [Evaluation Study Research Support, N. I.H., Extramural]. 2013;29:15–21.

18. McCarthy DJ, Campbell KR, Lun AT, Wills QF. Scater: pre-processing, quality control, normalization and visualization of single-cell RNA-seq data in R. Bioinformatics . 2017;33:1179–86. 15.

19. Kiselev VY, Kirschner K, Schaub MT, Andrews T, Yiu A, Chandra T. et al. SC3: consensus clustering of single-cell RNA-seq data. Nat. Methods. 2017;14:483–6.

20. Chal J, Al Tanoury Z, Oginuma M, Moncuquet P, Gobert B, Miyanari A, et al. Recapitulating early development of mouse musculoskeletal precursors of the paraxial mesoderm in vitro. Development. [Research Support, Non-U.S. Gov't]. 2018; 19:145:dev157339.

21. Papapetrou EP, Schambach A. Gene insertion into genomic safe harbors for human gene therapy. Mol Ther. 2016;24:678–84. [Research Support, N.I.H., Extramural Research Support, Non-U.S. Gov't. Review].

22. Holvoet B, Quattrocelli M, Belderbos S, Pollaris L, Wolfs E, Gheysens O. et al. Sodium iodide symporter PET and BLI noninvasively reveal mesoangioblast survival in dystrophic mice. Stem Cell Rep. 2015;5:1183–95. [Research Support, Non-U.S. Gov't]8.

23. Costamagna D, Quattrocelli M, van Tienen F, Umans L, de Coo IF, Zwijsen A. et al. Smad1/5/8 are myogenic regulators of murine and human mesoangioblasts. J Mol Cell Biol. 2016;8:73–87. [Research Support, Non-U.S. Gov't].

24. Ordovas L, Boon R, Pistoni M, Chen Y, Wolfs E, Guo W. et al. Efficient recombinase-mediated cassette exchange in hPSCs to study the hepatocyte lineage reveals AAVS1 locus-mediated transgene inhibition. Stem Cell Rep. 2015;5:918–31. [Research Support, Non-U.S. Gov't]10.

25. Lachmann A, Torre D, Keenan AB, Jagodnik KM, Lee HJ, Wang L. et al. Massive mining of publicly available RNA-seq data from human and mouse. Nat. Commun. 2018;9:1366 [Research Support, N.I.H., Extramural]10.

26. Quattrocelli M, Swinnen M, Giacomazzi G, Camps J, Barthelemy I, Ceccarelli G. et al. Mesodermal iPSC-derived progenitor cells functionally regenerate cardiac and skeletal muscle. J Clin Invest. 2015;125:4463–82. [Research Support, Non-U.S. Gov't].

27. Armstrong JPK, Keane TJ, Roques AC, Patrick PS, Mooney CM, Kuan WL, et al. A blueprint for translational regenerative medicine. Sci Transl Med. [Review]. 2020; 2;12:eaaz2253.

28. Kwon S, Ki SM, Park SE, Kim MJ, Hyung B, Lee NK. et al. Anti-apoptotic effects of human Wharton's jelly-derived mesenchymal stem cells on skeletal muscle cells mediated via secretion of XCL1. Mol. Ther. 2016;24:1550–60.

29. Potier E, Ferreira E, Andriamanalijaona R, Pujol JP, Oudina K, Logeart-Avramoglou D. et al. Hypoxia affects mesenchymal stromal cell osteogenic differentiation and angiogenic factor expression. Bone. 2007;40:1078–87.

30. Kim J, Magli A, Chan SSK, Oliveira VKP, Wu J, Darabi R. et al. Expansion and purification are critical for the therapeutic application of pluripotent stem cell-derived myogenic progenitors. Stem Cell Rep. 2017;9:12–22. [Research Support, N.I.H., Extramural Research Support, Non-U.S. Gov't]11.

31. Savelli S, Trombi L, D'Alessandro D, Moscato S, Pacini S, Giannotti S. et al. Pooled human serum: a new culture supplement for bioreactor-based cell therapies. Preliminary results. Cytotherapy. 2018;20:556–63. [Research Support, Non-U.S. Gov't].

32. Thaweesapphithak S, Tantrawatpan C, Kheolamai P, Tantikanlayaporn D, Roy-trakul S, Manochantr S. Human serum enhances the proliferative capacity and immunomodulatory property of MSCs derived from human placenta and umbilical cord. Stem Cell Res Ther. 2019;10:79 [Research Support, Non-U.S. Gov't]7.

33. Punzon I, Mauduit D, Holvoet B, Thibaud JL, de Fornel P, Deroose CM. et al. In vivo myoblasts tracking using the sodium iodide symporter gene expression in dogs. Mol Ther Methods Clin Dev. 2020;17:317–27. 12.

34. Sampaolesi M, Blot S, D'Antona G, Granger N, Tonlorenzi R, Innocenzi A. et al. Mesoangioblast stem cells ameliorate muscle function in dystrophic dogs. Nature. 2006;444:574–9. [Research Support, Non-U.S. Gov't]30.

35. Duan Q, Li S, Wen X, Sunnassee G, Chen J, Tan S, et al. Valproic acid enhances reprogramming efficiency and neuronal differentiation on small molecules staged-induction neural stem cells: suggested role of mTOR signaling. Front Neurosci. 2019;13:867.

36. Huangfu D, Maehr R, Guo W, Eijkelenboom A, Snitow M, Chen AE. et al. Induction of pluripotent stem cells by defined factors is greatly improved by small-molecule compounds. Nat Biotechnol. 2008;26:795–7. [Research Support, Non-U.S. Gov't].

37. Bettica P, Petrini S, D'Oria V, D'Amico A, Catteruccia M, Pane M, et al. Histological effects of givinostat in boys with Duchenne muscular dystrophy. Neuromuscul Disord. 2016;26:643–9.

38. Breuls N, Giacomazzi G, Sampaolesi M. (Epi)genetic modifications in myogenic stem cells: from novel insights to therapeutic perspectives. Cells. [Research Support, Non-U.S. Gov'tReview]. 2019; 9;8:429.

39. Alexander MS, Rozkalne A, Colletta A, Spinazzola JM, Johnson S, Rahimov F. et al. CD82 is a marker for prospective isolation of human muscle satellite cells and is linked to muscular dystrophies. Cell Stem Cell. 2016;19:800–7. [Research Support, N.I.H., Extramural Research Support, Non-U.S. Gov't]1.

AUTHOR CONTRIBUTIONS
N.B.: Conceptualization, methodology, formal analysis, investigation, writing—original draft and visualization. N.G. and L.Y.: writing—review and editing, validation. G.M.G.: in vivo experiments—writing. P.C.: methodology, writing—review and editing. S.H.: resources and writing—review and editing. A.R.: resources and writing—review and editing, C.D.: supervision, resources, and writing—review and editing, M.S.: supervision, conceptualization, funding acquisition and writing—review and editing.

COMPETING INTERESTS
The authors declare no competing interests.

ETHICS STATEMENT
All animal procedures were performed according to the guidelines of the Animal Welfare Committee of KU Leuven (Ethical Committee approval numbers P004/2017 and P182/2018) and Belgian/European legislation.

ADDITIONAL INFORMATION
Supplementary information The online version contains supplementary material available at https://doi.org/10.1038/s41419-021-03936-w.

Correspondence and requests for materials should be addressed to M.S.

Reprints and permission information is available at http://www.nature.com/reprints

Publisher's note Springer Nature remains neutral with regard to jurisdictional claims in published maps and institutional affiliations.